MMA Memo 201: Hour Angle Ranges for Configuration Optimization

M.A. Holdaway
National Radio Astronomy Observatory
949 N. Cherry Ave.
Tucson, AZ 85721-0655
email: mholdawa@nrao.edu

February 25, 1998

Abstract

As a source is tracked to lower and lower elevations, the atmospheric opacity increases the system temperature rather dramatically, especially at submillimeter wavelengths. We find that configurations of 850 m or smaller can achieve excellent (u,v) coverage in under two hours of observations (the smallest arrays have complete (u,v) coverage in a snapshot), but the 3000 m configuration requires about eight hours to achieve excellent (u,v) coverage. We investigate reasonable hour angle ranges which result in minimal sensitivity loss for observations over the range of declinations accessible to Chajnantor at frequencies of 225, 345, and 875 GHz for each of the quartile opacity conditions. Typically, hour angle limits of 2-3 hours (ie, 4-6 hours total observing) are possible without increasing the system temperature too much. Since most configurations do not require long tracks to achieve good Fourier plane coverage, and the atmosphere discourages long tracks on sensitivity grounds, long sensitive integrations will require many short observations near transit spread out over many days.

1 Snapshots, Full Tracks, and Array Optimizations

A number of researchers have implemented algorithms to optimize interferometric array configurations subject to some prior assumptions, but usually for only a snapshot at the zenith (Cornwell, 1986; Keto, 1997; Kogan, 1997, 1998). There is a simple transformation (stretching and rotating) between the zenith snapshot Fourier plane coverage and the snapshot coverage at any other point on the sky, so optimizing at the zenith will also optimize for any transit observation (ie, Kogan, private communication, 1998), except for beam elongation issues.

The MMA's compact arrays will be used primarily for mosaicing, which requires array optimizations for snapshots close to transit[1]. The MMA's large arrays will mainly be used for longer track integrations of single (or a few) fields. However, to date only one group has attempted to optimize a configuration over long track observations: Holdaway, Foster, and Morita (1996) found that the Keto algorithm, when modified to treat long tracks, produced declination dependent, non-triangular arrays.

In general, an array optimized for long tracks at one declination will not be optimal for sources at other declinations. To further illustrate this point, consider Kogan's algorithm, which seeks to minimize the peak sidelobe level within some region of the point spread function for a zenith snapshot. Part of the sidelobe reduction is accomplished through the tapered envelope of the Fourier plane coverage. Kogan's new algorithm produces "donut" arrays, and the width of the taper in the Fourier plane is directly related to the width of the donut. Now consider long track observations of a source at dec = 0. The baselines

[1]We cannot use any of the canned optimizations for the compact arrays as we have more requirements to consider; see Helfer and Holdaway, 1998.

Freq [GHz]	$T_\circ$ [K]
90	31.6
225	61.4
345	84.8
675	155.8
875	198.8

Table 1: Zero opacity system temperatures for the MMA at various frequencies.

will experience foreshortening in the E-W direction when the source is at low elevation, and the Fourier plane coverage is effectively tapered in the E-W direction through this foreshortening. If we were to optimize for long tracks at dec = 0, this foreshortening tapering will result in a reduced need for the taper which results from the thickness of the donut, at least in the E-W direction. Hence, the resulting configuration should be a donut which is thicker on the north and south, and thinner on the east and west. The longer the tracks, the thinner the donut would become in the east and west. Now, if we optimized for long tracks at different declinations, the foreshortening would occur in both E-W and N-S directions, in varying amounts depending on the declination and hour angle range, resulting in different array configurations.

So, once we decide to open up the question of optimizing for long track optimizations, we must also address optimizing over all declinations as well. However, all declinations are not created equal. First, the distribution of sources which we wish to observe is a complicated function of declination, including contributions from solar system, galactic, nearby and distant extragalactic sources, each with their unique distributions with declination (Holdaway *et al.*, 1996.) Second, sources at different declinations really require different length tracks on the sky, mainly due to the different effects of atmospheric opacity on source tracks at different declinations. For a Millimeter Array at the Chajnantor site, we estimate the typical hour angle range over which it is profitable to observe a source as a function of declination.

2 System Temperature and Elevation

Assume that the effective system temperature depends upon elevation only through the atmospheric opacity. This will not be exactly correct, as spill over efficiencies will depend upon elevation angle too, especially at the higher frequencies where the telescope is not as precise as we would like it to be. M.P. Rupen has provided estimates of the *zero opacity* system temperature $T_\circ$, which are given in Table 1 (we won't go into detail about where these numbers come from, as they will be the subject of an in depth memo on the MMA sensitivity; but we will point out that these numbers correspond to a single sideband receiver temperature of 4.5 $h\nu/k$, which is perceived as the optimistic value which the MMA receivers will eventually be able to achieve).

We assume that the effective system temperature at an air mass of m is given by

$$T_{sys}(m,\nu) = \left(T_\circ(\nu) + T_{sky}(1 - e^{-m\tau(\nu)})\right) e^{m\tau(\nu)}.$$

We use the 225 GHz tipping radiometer database from Chajnantor to give us first, second, and third quartile zenith opacities at 225 GHz. To estimate the quartile opacities at other frequencies, we use the empirical relationships between the opacities at 220 GHz and higher frequencies as obtained by Matsuo *et al.* (1998) with their FTS tipper. These relationships are shown in Table 2. Matsuo *et al.* caution that knowledge of the 220 GHz opacity does not uniquely specify the submillimeter opacity, but our analysis is only statistical, and the given linear relationships suffice for our purposes. Side by side measurements with the NRAO 225 GHz radiometer and the NRO 220 GHz radiometer indicate that the atmospheric opacity is essentially the same at these two close frequencies. Hence, we are justified in combining our

Freq [GHz]	a	σ_a	b	σ_b
90	0.133	0.00	0.013	0.000
345	3.54	0.05	0.001	0.006
675	20.7	0.7	0.063	0.075
875	22.1	0.8	0.072	0.090

Table 2: Relationships between 220 GHz opacity and the opacity at other frequencies as determined by Matsuo *et al.* (1998): $\tau_\nu = a_\nu * \tau_{220} + b_\nu$. The 90 GHz parameters were determined by the Liebe model, as the FTS tipper did not go as low as 90 GHz.

quartile 225 GHz opacities with the relationships scaling from 220 GHz to obtain estimates of the opacities at different frequencies.

We have used the geometry subroutines in SDE to compute the hour angle/elevation tracks of sources at various declinations, calculating the effective system temperature for every 60 s point on these tracks, down to the 5° elevation limit of the MMA antennas. The airmass m is estimated to be $1/\sin(e\ell)$.

3 Observing Philosophy

Figure 1 shows an example of how the relative data weight (defined as $1/T^2_{sys}$, normalized to a zenith weight of 1.0 for each frequency and atmospheric condition) degrades with hour angle for different frequencies. Consider one observation taken at a weight of 1.0, and another taken at a weight of 0.5. If the observations were of equal duration, the second would yield a SNR $\sqrt{2}$ worse than the first. Or, if we sought equal SNR, we would have to observe for twice as long for the second observation. Typically, the weight decreases to 0.5 between 2 and 5 hours off of transit, depending upon observing frequency, source declination, and atmospheric opacity.

3.1 How will the MMA be used?

If we look to existing millimeter wavelength interferometers, we see that they are generally scheduled in long (ie, 8 hour) tracks. This inevitably results in wasting a great deal of time integrating with very high system temperature. If the weights are calculated correctly and used correctly in the imaging, then these long tracks will be only a little more sensitive than much shorter integrations. If the weights are not handled correctly, then these long tracks will actually degrade the SNR of the final images. So, why are long tracks still used, rather than multiple shorter tracks? The long tracks do improve the Fourier plane coverage, which is especially important for the current generation of millimeter wavelength interferometers. (How much the Fourier plane coverage is improved is an open question, as the effect of low weight Fourier samples on image quality has not been investigated. However, it is a given that the only way to get certain Fourier samples in certain configurations is to observe long tracks at lower than desired elevations.) However, another reason is that astronomers don't want to deal with several short track observations made on different days, even if the SNR is much better. The multiple observations each need to be calibrated, and cross calibrated to ensure that the flux scale is consistent among the different data sets. However, if the MMA performs the calibration (and even the imaging) as a service to the astronomical community (ie, Scott *et al.*, 1996; Holdaway, 1997), then there is no drawback to observing a given source on multiple near-transit tracks, aside from the Fourier plane coverage issue.

3.2 The MMA's Fourier Plane Coverage

The Fourier plane coverage issue can be addressed through the "fraction of occupied cells" (FOCC, Morita, 1997). The FOCC is calculated by simulating (u, v) points for a given MMA configuration with short integration time (ie, 10 s) and gridding them onto a Fourier plane with cell size 10 m (ie, the dish diameter); within a circular mask with radius equal to the array size, we calculate the ratio of cells with at least one Fourier sample to the total number of cells. The FOCC is calculated as a function of hour angle limit for 250, 850, and 3000 m 36 element configurations in Figure 2. A rule of thumb is that imaging of large, complex objects is fairly poor when the FOCC is less than about 0.5. Figure 2 shows that the smaller configurations start out in snapshot mode with a high fraction of occupied cells and increase slowly (ie, partially redundantly) until they saturate near 1.0 for longer track observations. The larger configurations start out with low FOCC for snapshots and increase more quickly with hour angle (ie, non-redundantly), and do not saturate so quickly. For the 3000 m configuration, we reach the 50% FOCC at 4 hours (ie, 8 hours of total observing), but the 850 m configuration reaches the 50% FOCC point at just over an hour. The 250 m configuration reaches the 50% FOCC point after only 10 minutes. It is interesting to note that the nonredundant FOCC is roughly proportional to

$$(nD/B_{max})^2,$$

where n is the number of antennas, D is the dish diameter, and B_{max} is the maximum baseline length in the array. Hence, to achieve optimal Fourier plane coverage, one wants to optimize the so-called "collecting length" nD. Since the MMA has changed from 40 x 8 m to 36 x 10 m, both the nD^2 and nD measures have increased, so the telescope design is better off, at least in the things that are easy to measure.

3.3 Implications for the MMA's Use Strategy

From a Fourier coverage point of view, the MMA could be used as a near-transit instrument (ie, from -1 to +1 hours of transit) in all arrays smaller than the 3000 m array. The 3000 m configuration (and the 10 km configuration, should it be built) need longer tracks for Fourier coverage reasons. How should the configurations be optimized? Since interest in the sky is not evenly distributed in right ascension (ie, the Galactic Center, Orion, etc.), there will be LST's of prime interest and some with less interest. So, practically the MMA will need to spend some time observing somewhat off-transit, even in the smaller configurations where good enough Fourier plane coverage can be obtained in a very short time very close to transit.

3.4 What Should be Optimized?

The 95 m and 250 m arrays should be optimized for snapshot coverage (as well as the other items mentioned in Helfer and Holdaway, 1998), but they must provide good snapshots somewhat off-transit, as determined by the hour angle-weight calculations. Beyond 3 hours off transit, the 95 m array will not be functional due to shadowing (Holdaway and Foster, 1996). The 850 m configuration should be optimized for 2 hour integrations both on transit and slightly off-transit, as determined by the hour angle-weight calculations. And the 3000 m configuration should be optimized for integrations as long as the hour angle-weight calculations sensibly permit.

4 Maximum Hour Angle Profiles

Figure 3 shows for several frequencies the hour angle as a function of declination at which the visibility weight drops to 50%, 65%, and 80% of its transit value for first quartile opacity conditions. Figures 4 and 5 show similar plots for second and third quartile opacity conditions. As can be seen, the hour angle limit gets smaller as the atmospheric opacity conditions worsen, as the frequency gets higher, and as the demand of high weight data increases. Near the celestial south pole, the hour angle range increases as the airmass does not change much with hour angle, and far northern sources have a decreased hour angle range because even modest hour angles result in a large increase in the airmass. However, to first order, many of the hour angle profiles are close to flat across many declinations.

We should mention two cases which require long integrations in the 3000 m array: sensitivity limited observations, and dynamic range limited imaging. (Remember that the other arrays will get sufficiently good Fourier plane coverage in a short enough time to be considered "snapshot" arrays, if we stretch the meaning of "snapshot" to include a 2 hour observation for the 850 m array.) Anyway, sensitivity limited observations do not require extremely good Fourier plane coverage: any old array with 36 elements not designed too pathologically will do. Sensitivity limited observations need not worry about long tracks, but can live with many short tracks taken near transit over several days. Dynamic range limited observations will actually require tracks to as low elevation as we can bear (probably to between 2 and 4 hours off transit, depending upon conditions, judging from Figures 3-5). It is true that if we build a *really bad* array, it will shift the point at which the imaging is dynamic range limited to lower SNR objects, this is probably not a big issue. Rather, if we optimize the 3000 m array for the longest sensible tracks, it will still be pretty good for snapshots and moderate length observations taken over many days for sensitivity limited observations.

References

Cornwell, T.J., 1986, "Crystalline Antenna Arrays", MMA Memo 38.

Helfer, Tamara and Holdaway, M.A., 1998, "Design Concepts for Strawperson Antenna Configurations for the MMA", MMA Memo 198.

Holdaway, M.A., 1997, "High Level Computing Information Flow for the MMA", MMA Memo 167.

Holdaway, M.A., and Foster, Scott M., 1996, "Evaluating the Minimum Baseline Constraints for the MMA D Array", MMA Memo 155.

Holdaway, M.A., Foster, S.F, and Morita, K.-I., 1996 "Fitting a 12km Configuration on the Chajnantor Site", MMA Memo 153.

Holdaway, M.A., *et al.*, 1996, "Wind Velocities at the Chajnantor and Mauna Kea Sites and the Effect on MMA Pointing", MMA Memo 159.

Keto, Eric, 1997, "The Shapes of Cross-Correlation Interferometers", ApJ 475, p. 843.

Kogan, L.R., 1998, *private communication.*

Kogan, L.R., 1997, "Optimization of an array configuration minimizing side lobes", MMA Memo 171.
Matsuo, Hiroshi; Sakamoto, Akihiro; and Matsushita, Satoki, 1998, "FTS measurements of submillimeter-wave opacity at Pampa la Bola", *submitted to PASJ.*

Morita, Koh-Ichiro, 1997, URSI proceedings.

Scott, Steve *et al.*, 1996, "MMA Computing Working Group Report", MMA Memo 164.

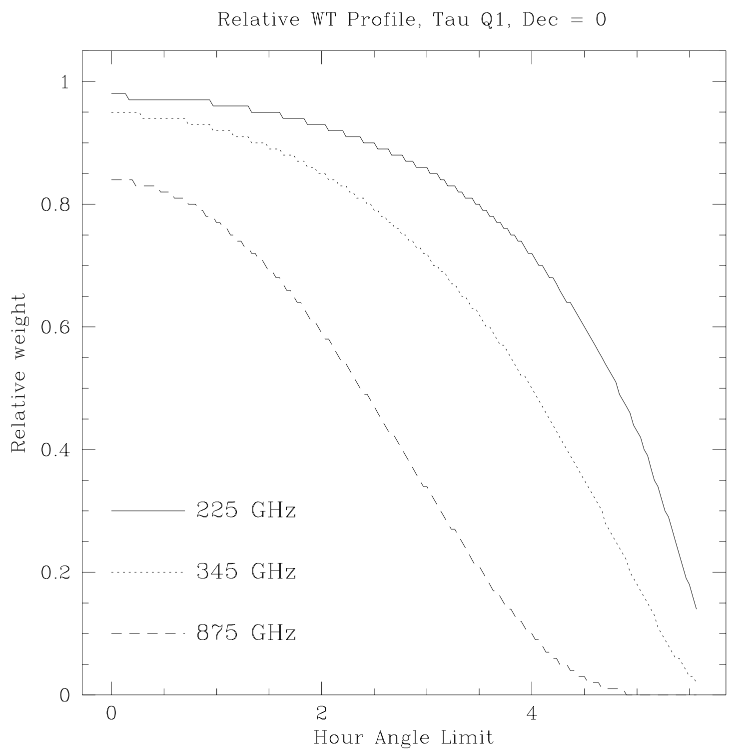

Figure 1: Visibility weight ($\propto 1/\sigma^2$), normalized such that WT=1.0 at zenith, for first quartile opacities, a source at dec = 0, and frequencies 225, 345, and 875 GHz.

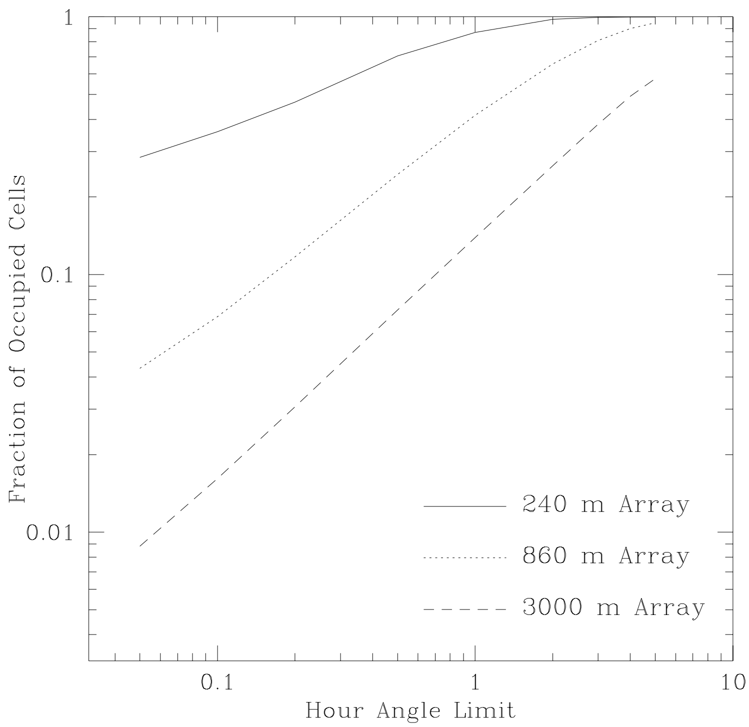

Figure 2: Fraction of occupied cells (FOCC) as a function of hour angle limit for 250 m, 850 m, and 3000 m configurations. A rule of thumb is that image quality for complicated sources is poor until FOCC is about 0.5. This figure indicates that there is something to be gained from long tracks for complicated objects, in spite of the increase in system noise.

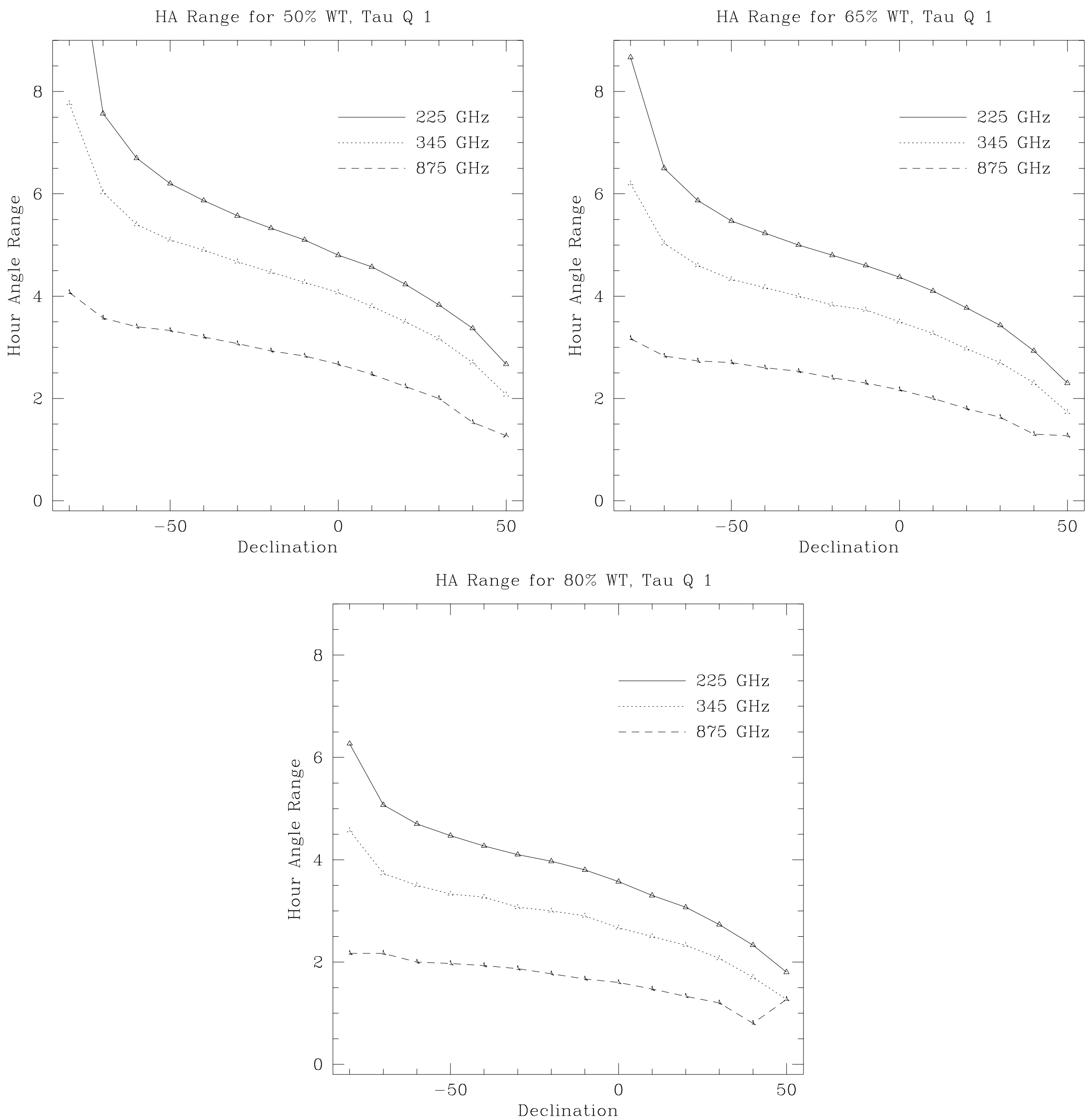

Figure 3: Hour angle at which WT is decreased to 50%, 65%, and 80% of its transit value, at 225, 345, and 875 GHz, first quartile opacities. Actual integration time will be twice the hour angle.

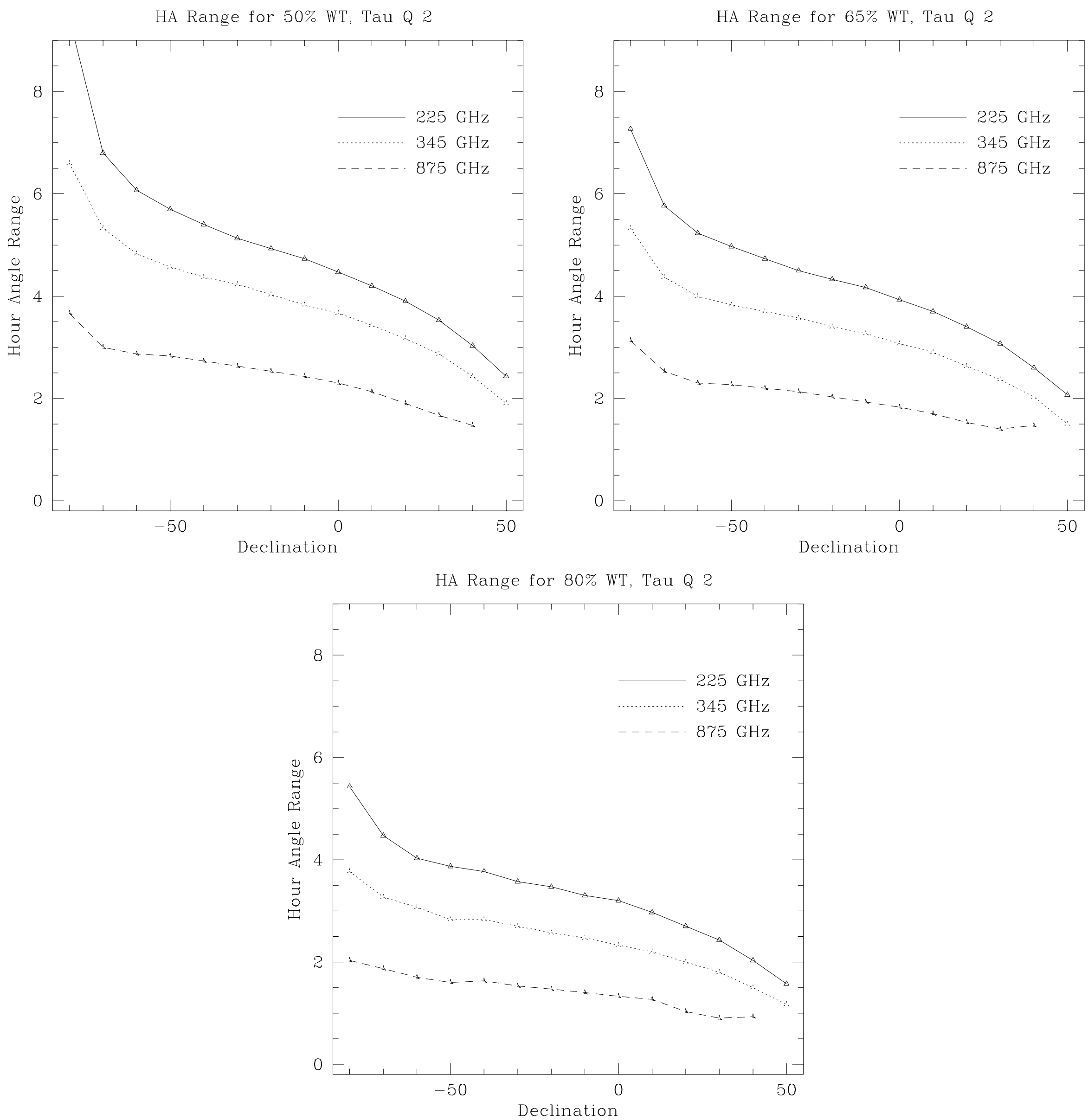

Figure 4: Hour angle at which WT is decreased to 50%, 65%, and 80% of its transit value, at 225, 345, and 875 GHz, second quartile opacities. Actual integration time will be twice the hour angle.

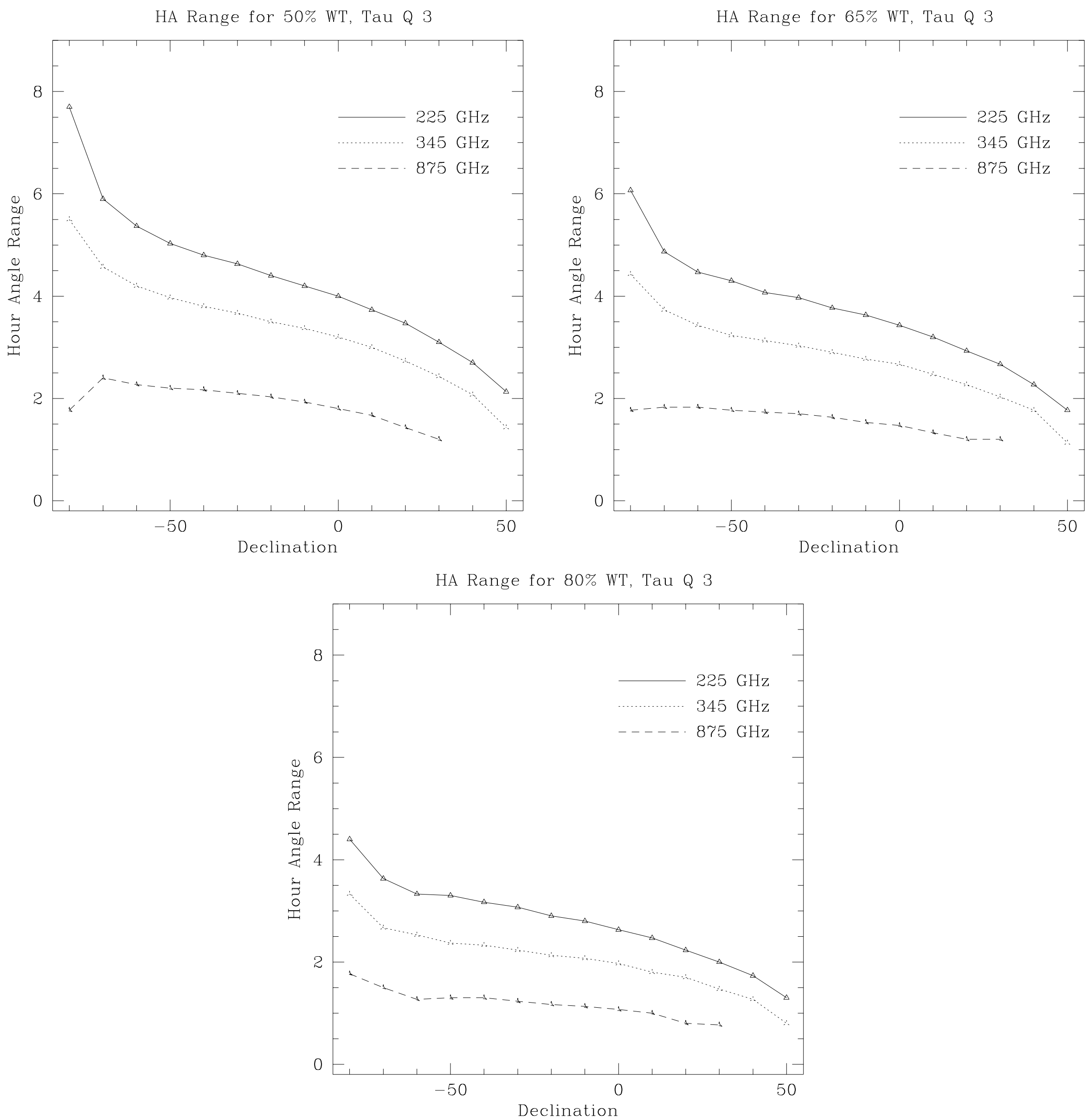

Figure 5: Hour angle at which WT is decreased to 50%, 65%, and 80% of its transit value, at 225, 345, and 875 GHz, third quartile opacities. Actual integration time will be twice the hour angle.